CHAPTER 3

METHODOLOGY

In this project, the design concerns and scopes of study for the MEMS microrelay are set to focus only at the mechanical path which is consisting a piezo actuator and a contact cross bar. Then, a specific application is set for Radio Frequency (RF) in telecommunication application due to ease the case study. However, the design of the mechanical path is designed to suit the universal applications. So, a single pole single throw of microrelay is designed to be switched vertically by a couple of single bimorph cantilever beam with the piezoelectric actuation method and a flat surface contact cross bar attached to it. Then, a RF signal line was put beneath the actuator and the cross bar. The methodologies of doing this project are presented from the designing stage through simulation for every part of it.

3.1 Process flow

The preliminary designs are done with the methodologies as presenting in the following section based on the specifications and concepts generated at the previous initial stages. Then, the preliminary designs are refined and undergo a detail analyses and CAD simulations in order to come out a definitive design. The whole process was summarized and attached as Appendix A.

Since, the design concerns only focus in the mechanical path of the microrelay including the actuator and the contactor. So, its geometry parameters, functions,

materials chosen, and others related issues are presented in the following section, and are made sure to be matched with the signal path.

3.2 Mechanical path design

The mechanical path is formed by two main elements which are the piezo actuator and a flat surface contact cross bar. The actuator is a multilayer sandwich bridge (fixed-fixed or double-clamped) consisting of a polysilicon as the beam elastic layer and a pair of bimorph electrodes in between a piezoelectric material. The overall structure is shown in figure 3.0(a).

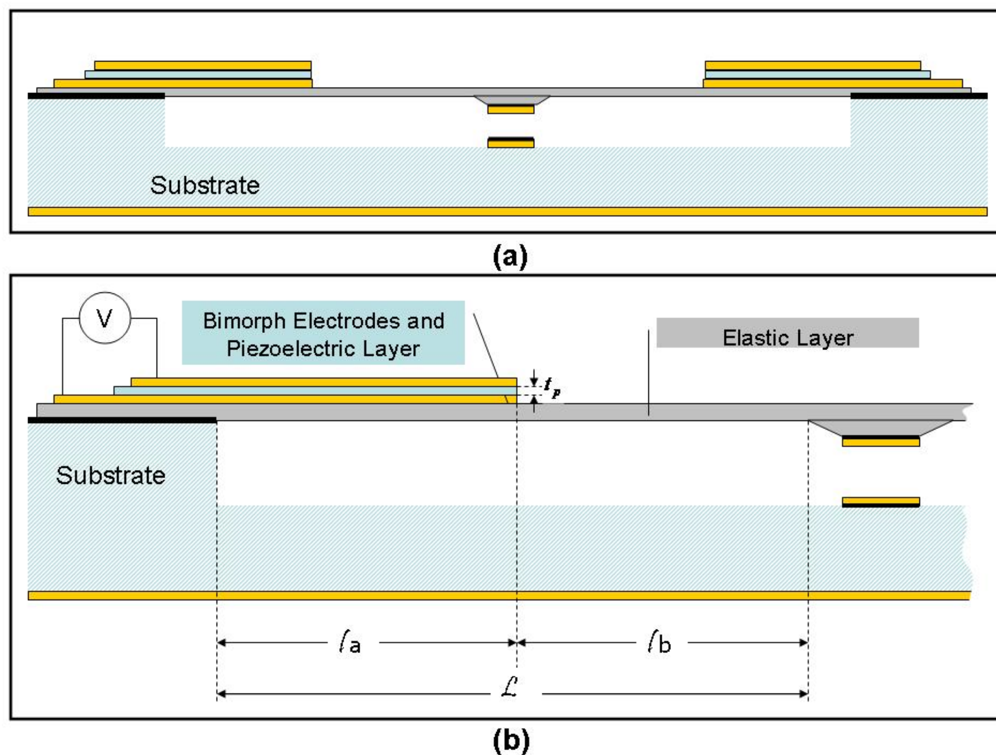

Figure 3.0: Cross sectional of microrelay. (a) Full model (b) Half model

There are actually two ways to classify this beam [4]. It can be considered as a fixed-fixed cantilever parallel to the substrate plane with a thick and stiff part in the middle. Alternatively, this beam can be considered as two fixed-guided beams jointed in

parallel to support a rigid part, as shown in figure 3.0. So, the methodology will begin with one fixed-guided beam as shown in figure 3.0(b) to ease the process of design, modeling and analysis through out the whole procedures in doing this project.

3.2.1 Bimorph cantilever piezo-actuator Model

First of all, analytical methods [4] are used in order to analyze the mechanical behaviors of the model and also to estimate the desire results to be generated from it. Beside that, it is also used in materials chosen and structure dimensions setting in order to get the desire stable displacement to suit into the microrelay specifications.

In this particular case as shown in figure 3.0(b), the polarization axis is perpendicular to the top surface of the cantilever and then the longitudinal direction is along to the length of the beam. The primary applied electric field is applied along the polarization axis as representing with the voltage supply symbol in figure 3.0(b). Furthermore, there is no mechanical stress presented, so the strain is only related to the electric field in this case. According to equation (2.1) if the longitudinal stress S_{long} is only related to electrical field E_3 without other external forces presented, it is possible to be simplified and representing as

$$S_{long} = d_{31} E_3 \tag{3.0}$$

Then, E_3 will be the electric field in polarization axis and given as

$$E_3 = \frac{V}{t_p} \tag{3.1}$$

After that, the radius of curvature, r can be found by plugging in the expression for S_{long} into equation (2.3). The vertical displacement at the end of segment denoted by l_a as shown in figure 3.0(b) can be found by using the equation (2.5) as $\delta(x = l_a)$. The angular displacement at the end of the piezoelectric patch is

$$\phi(x = l_a) = \frac{l_a}{r} \tag{3.2}$$

The segment denoted by l_b does not curl and remain straight. So that, the maximum vertical displacement at the end of the beam can be estimated as

$$\delta(x = L) = \delta(x = l_a) + l_b \sin[\phi(x = l_a)] \tag{3.3}$$

Then, the plots for displacements versus material types, structure dimensions and actuation voltages can be easily plotted with aids of MathCAD for further analysis. Due to limit and ease the analysis, selected materials such as PZT-4, Zinc Oxide (ZnO) and Quartz from piezoelectric materials, and the polycrystalline silicon (polysilicon) and silicon nitride as the elastic materials will only be concerned. An analyzer developed by using MathCAD is also attached in appendix B as Mechanical Displacement Analyzer. Then the analysis results for two piezoelectric materials are presented as following in figure 3.1.

3.2.2 Selection of materials

Quartz is not considered in this design as the suitable piezoelectric material because it delivers very low effect in actuation displacement compare to ZnO and PZT. Base on the result from figure 3.1 and the material properties in appendix C, PZT is the one with highest piezoelectric coupling and deform the most in the same condition for a fixed dimension. However, ZnO is chosen as the best suit material for this project due to it's insensitive to temperature change and capable to deform as low as 5V for about 2μm displacement gap while switching. The piezoelectric coefficient matrix for ZnO [4] is

$$d = \begin{bmatrix} 0 & 0 & 0 & 0 & -11.34 & 0 \\ 0 & 0 & 0 & -11.34 & 0 & 0 \\ -5.43 & -5.43 & 11.37 & 0 & 0 & 0 \end{bmatrix} \times 10^{-12}\,\text{C/N} \tag{3.4}$$

ZnO material can be grown using a number of methods, including RF and DC sputtering, ion plating, and chemical vapor deposition [4]. In MEMS field, ZnO is most commonly deposited by magnetron sputtering with the c-axis is spontaneously formed without pulling which is been reported by some other researchers in their journals since

1980. As-deposited ZnO films have significant compressive stress ranging from 1GPa to 135GPa. The stress can be reduced using thermal annealing at 500˚C for about 5 minutes n the 80MPa to 100MPa range. Since aluminum is the popular electrode material on top of the ZnO thin film, so it is chosen to be used in this design for the cost concerns while it has lower cost compare to gold.

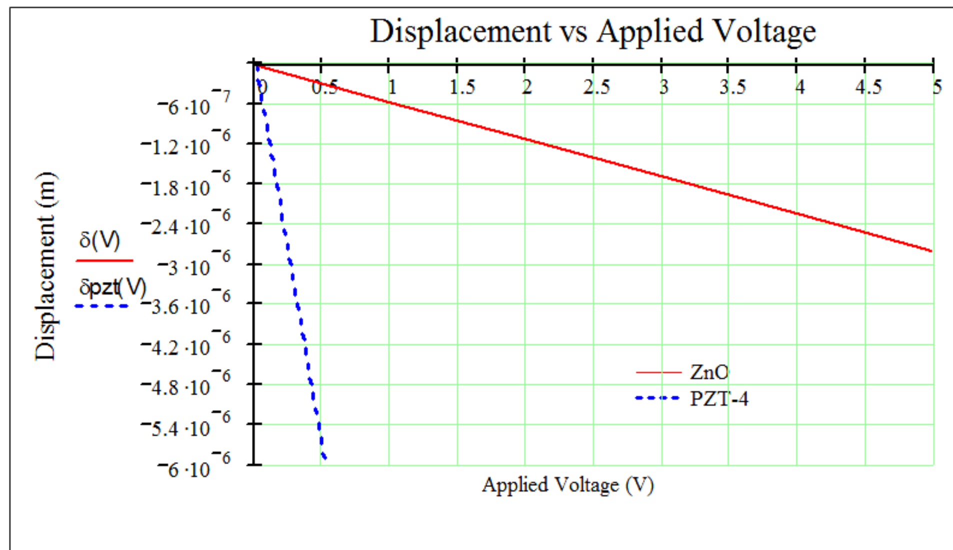

Figure 3.1: Actuator displacements of various piezoelectric materials

By using the same method, polysilicon is chosen as the elastic beam material from silicon nitride. The analyzer showed that polysilicon has the capability to displace at lower actuation voltage compare to silicon nitride for a fixed dimension and a same piezoelectric material. The analytical result showed that the single bimorph cantilever structural with ZnO as the actuation layer, the displacement of the tip beam can be reach up to 2.8μm at 5V.

3.2.3 Bridge structural

After material selection and dimension setting for the desire geometry structural, the single cantilever beam actuator is then being considered to put it in array configuration where two cantilevers are placed in the opposite side respectively and

separated with a contactor at the middle to form a bridge structure as shown in figure 3.0(a). In other word, both fixed-guided beams are jointed in parallel to support the rigid part with higher force constant in order to prevent the beam initial condition from over bending as shown in figure 3.2(a) and 3.2(c).

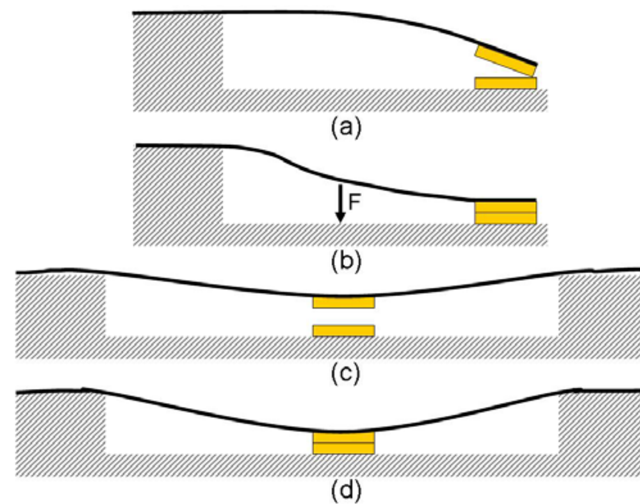

Figure 3.2: Effect of various actuators configurations. (a) Cantilever initial condition, (b) Cantilever loaded condition, (c) Bridge initial condition, (d) Bridge loaded condition

There are several reasons in use of the bridge structural instead of using the single cantilever bimorph beam. Firstly, piezoelectric actuation method is used to force the beam to bend down by using its longitudinal stress along the length of the beam. A curvature bend generated is then hence increasing the possibility to have an imperfect contact as shown in figure 3.2(a). Then, the on-resistance will be increased and lower down the ability to withstand current gauge. Base on some research papers, if electrostatic extraction force applying as denoted by F in figure 3.2(b), the beam of the actuator will be deformed in S-shaped and hence an even contact force to make a full close contact. Unfortunately, this is only applicable to metal thin membrane. Beside that, modifying the beam end due to have a good contact will involve other complicated concerns. So, the concept of using array configuration to form a bridge structure as shown in figure 3.2(c) is considered eventually in order to have a good contact as shown in figure 3.2(d). Beside that, it also to reduce the beam vibration degree while return to the initial position. Furthermore, this method also eases the development process later since it not involving any additional micro fabrication step.

3.2.3.1 Force constant

A two dimensional fixed-guided beam is considered with movement confined to one plane. Each point along the length of the beam can have a maximum of two linear degrees of freedom (DOF) and null in rotational degree of freedom. The force constant or stiffness coefficients of a fixed-guided beam [4] as shown in figure 3.0(b) is given as

$$K = \frac{CE_B I_B}{L^3} \tag{3.5}$$

where the C is a coefficient that depend on the beam-loading and boundary condition. For the beam-bending situation such as fixed-guided beam its C value is equal to 12. Since the bridge structural is form with two cantilevers beam as mentioned before, and the combination of these two beams structural is equivalent to parallel stiffness connection [4] [14]. The total coefficient is given as

$$K_{Bridge} = K_1 + K_2 = 2\frac{CE_B I_B}{L^3} \tag{3.6}$$

Then, the force generated from piezoelectric material to bend down the beam can be found by applying the Hooke's Law, which states that the force with the spring (beam) pushes back is linearly proportional to the distance from its equilibrium length [17]. The amount of force achievable equals the force required to restore the beam to its initial un-deformed state.

$$F = -K_{eq} \cdot \delta(x) \tag{3.7}$$

where the K_{eq} is the equivalent stiffness coefficient for the system. Basically the maximum displacement of the bridge structure will be lesser than the single cantilever beam displacement due to its higher stiffness coefficient. So, higher actuation voltage is required for the bridge structure to deliver the same displacement in order to make a perfect contact with equivalent force.

3.2.3.2 Driving voltage

The next consideration in designing the mechanical path is to estimate the actuator driving voltage. A good design should have the lowest actuation voltage, but

increasing of the force constant for the bridge structural compares to cantilever beam with ratio 2:1 given by equation (3.6) has lead to increase the require driving voltage. The estimation of the minimum voltage requirement to make a 2μm displacement is shown as in figure 3.3. The assumption made due to the ratio of force constants and Hooke's Law, where was given in equation (3.7). For a fixed displacement and greater bridge structural force constant, then a greater force will be needed for the actuation. So, higher driving voltage must be applied in order to generate the require force. Figure 3.3 shows that the driving voltage for bridge structural one time greater than the cantilever beam actuator.

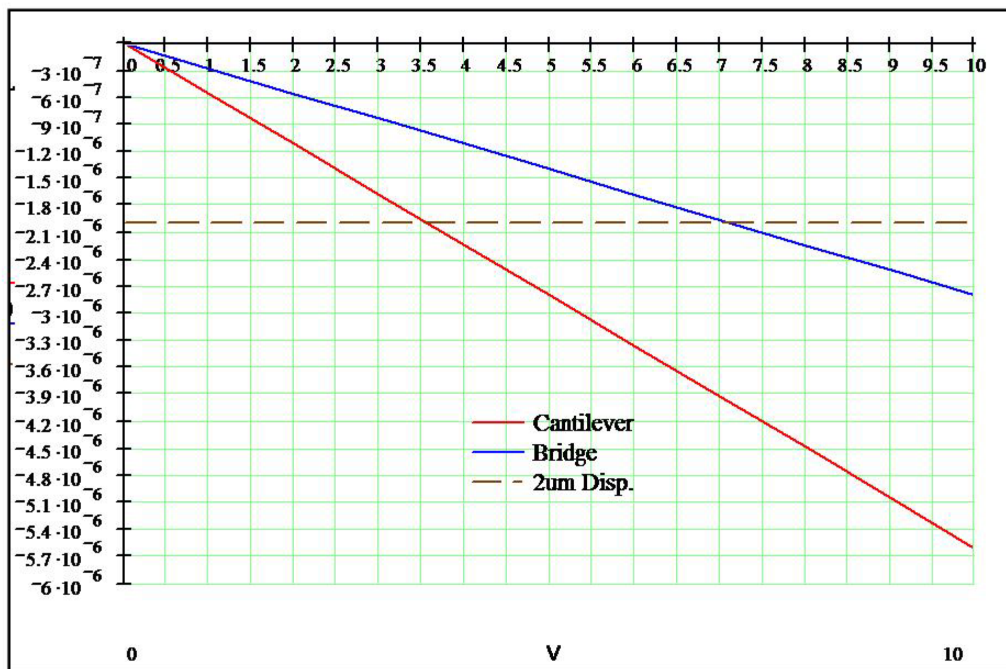

Figure 3.3: Driving voltage of various configuration piezo-actuators

3.2.3.3 Resonant frequency and quality factor

At low frequency, the displacement remains constant [4]. This represents the low frequency behavior that applies to the steady loading case. At or near the resonant frequency, f_n the mechanical vibration amplitude sharply increases. The sharpness of the resonant peak is characterized by a term called the quality factor, Q. The sharper the

resonance peak, the higher the quality factor. The amplitude magnification at the resonant frequency can be beneficial. Operating a micro sensor or actuator at the resonant frequency may increase the sensitivity or range of actuation. However, resonance may also lead to the self-destruction of mechanical elements.

The quality factor [4], representing the sharpness of resonance peaks, can be defined in several ways. Form the energy point of view; it is the ratio of the total stored energy in system over the energy lost over each cycle of oscillation. The lower the energy loss per cycle, the greater the quality factor. Some common forms of energy loss include mechanical energy dissipation into the substrate through anchors, mechanical damping by surrounding media (e.g., air), and thermal elastic energy dissipation or internal friction.

Mathematically, the quality factor is related to the full width at half maximum (FWHM), which is the spacing of two frequencies at half power (or 77% amplitude). The ratio of the resonant frequency and the FWHM gives the quality factor:

$$Q = \frac{f_n}{\Delta f} \tag{3.8}$$

The resonant frequency of simplest mechanical system is given by

$$f_n = \frac{\omega_n}{2\pi} = \frac{1}{2\pi}\sqrt{\frac{K}{M}} \tag{3.9}$$

where the mass, M can be found by multiply the volume with its mass density.

3.2.4 Flat surface contact cross bar

The design of a microrelay actuator has to be based on the characteristic data of the contact material used. So, gold (Au) is chosen as the contact metal because of its low resistivity, good stability and efficiency in RF signal propagation. Its skin depth can be calculated [18] by

$$\delta = \frac{1}{\sqrt{f 2\pi\sigma}} = \sqrt{\frac{\rho_{Au}}{\pi\mu_0 f_s}} \tag{3.10}$$

Where the resistivity of gold ρ_{Au} =0.1Ω-µm and $\mu_o = 4\pi \times 10^{-7} H/m$. The conductor resistance, R [14] given by

$$R = \frac{\rho_{Au} L}{A} \tag{3.11}$$

The geometry shape of the contactor is chosen as a rectangle box in order to have a flat-to-flat surfaces contact with the signal path. According to Jin Qiu, none of the various geometry contact surfaces other than flat-flat type given a good contact resistance as being reported in the research paper of An Electro Thermally Actuated Bistable MEMS Relay for Power Applications [8]. Then, due to have a perfect closure between the cross bar and the signal path, a rigid path to form a guided contact bar is necessary to be created by using a various thickness of beam as shown in figure 3.0 where there is a thicker portion at the center of the beam. This rigid path will be preventing curvature bend at the bar while to make a contact.

3.3 Signal path analysis

The signal path is the core element in determine the applications of a microrelay. Since RF MEMS was chosen as the project scope of study, so RF signals lines are considered here. Because of the CAD software in UniMAP MEMS design laboratory do not support in designing and analysis the RF devices, so an existing design is chosen as W-Band Finite Coplanar Waveguide (FGCPW) to Microstrip Line Transition done by a group of researchers in 1998 [19].

The design is uni-planar and does not require via holes or wire bonds. The transition, centered at 94GHz, results in 0.2dB insertion loss with a bandwidth of 20%. The return loss is better than -17dB from 85GHz to 100GHz. The input line is a 50Ω finite ground coplanar waveguide (FGCPW) and the output line is a 50Ω microstrip line as shown in figure 3.4.

The transitions are to be built on about 100µm thick high-resistivity silicon substrate (ε_r = 11.7). The circuit is to be mounted on a metallized silicon wafer to provide the infinite ground plane. The FGCPW input line dimensions are S2=50µm, W2=45µm and G2=145µm corresponding to a characteristic impedance of Zo=47Ω. The misrostrip line is 74µm, corresponding to a characteristic impedance of Zm=50Ω. The coupling region is chosen to be L=280µm long (λs/4 at 94GHz) and the dimensions are S1=30µm, W1=55µm, and the straight stubs are G1=45µm wide, corresponding of fundamental mode impedance of Z_{oo}=13Ω, Z_{oe}=130Ω and Z_{ee}=50Ω.

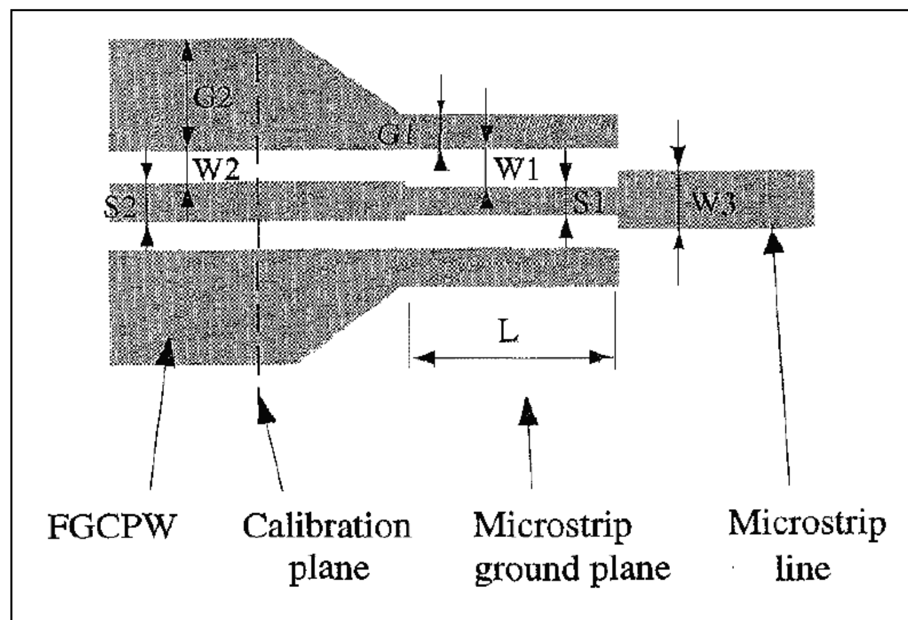

Figure 3.4: CPW-to-microstrip transition with straight coupling stubs [19]

However only part of the FGCPW layout is model again by using Layout Editor (LEdit) of MEMS Pro CAD software which is a pair of microstrip line with 380µm length and separated with gap of 150µm. After that, a full 3D model was then be generated together with mechanical path as shown in appendix E-G. The portion of RF signal line was analyzed by using a microwave calculator from [21] and its given 51.537 Ω impedance and 7.665 in effective permittivity as shown in appendix D.

The material chosen for the signal path is gold, where the evaporated gold about 9000Å thick will give about 3 skin depth at 94GHz [19]. However, aluminum

transmission lines have been presented at [22]. The thick aluminum metallization system is compatible with CMOS circuitry and exhibits low losses at high frequency. The losses of these aluminum transmission lines are on the order of 0.06dB/mm at 10GHz. Therefore, aluminum may consider reducing the cost charge for suitable applications. For further details information in design, applications and other technical concerns can be obtained from [19-22].

3.4 Layout generation and 3D modeling

Basically, it is the layout generation process and 3D modeling of the devices by using computer aided design tools. The CAD modeler used to create the virtue prototype is MEMS Pro Layout Editor (LEdit). CAD modeling is begun with layer definition and then follows with 2D layout drawing as shown in appendix E for the full layout of microrelay. After the layout passes the Design Rules Checks, DRC, the 3D model is generated base on the defined processes as in table 3.1 and its material properties set as shown in appendix C. A completed 3D model will then be converted and exports in iges. format file to solver fro further simulations and analysis.

Table 3.0: 3D CAD Modeling Process Summary

App. Proc. No	Label / Mask	Command	Mask Type	Face	Target / Etch Remove	Thickness (μm<θ˚)
1	Substrate	Wafer			Si <100>	100
1	Beam Anchor	Etch: Wetaniso	Outside	T	Si <100>	4<90
2	Isolation Oxide	Deposit: Snow Fall		T	SiO2	2
3	Signal Line	Deposit: Snow Fall		TB	Au	0.9
4	Top Line	Etch: Dry	Outside	T	Au	0.9<90

5	Sacrificial	Deposit: Fill		T	Polymide	1
5	Contact Hole	Etch: Dry	Inside	T	Polymide	2<90
6	Au Contact	Deposit: Snow Fall		T	Au	1
6	Pattern Contact	Etch: Dry	Outside	T	Au	1<90
7	Beam Clamp	Etch: Dry	Inside	T	Polymide	1<45 (UC1)
8	Bar Iso	Deposit: Snow Fall		T	SiO2	0.5
8	Pattern Bar Iso	Etch: Dry	Outside	T	SiO2	0.5<90
8	Contact Hole 2	Etch: Dry	Inside	T	Polymide	1<45 (UC0.5)
9	PolyBeam	Deposit: Fill		T	Polysilicon	1
9	Pattern Beam	Etch: Dry	Outside	T	Polysilicon	2<90
10	Bot Electrode	Deposit: Snow Fall		T	Al	0.5
10	Pattern BotE	Etch: Dry	Outside	T	Al	0.5<90
11	Piezo	Deposit: Snow Fall		T	ZnO	0.5
12	Top Electrode	Deposit: Snow Fall		T	Al	0.5
12	Pattern TopE	Etch: Dry	Outside	T	Al	0.5<90
13	Pattern Piezo	Etch:d	Outside	T	ZnO	5<90
14	Free	Etch: Sacrificial		T	Polymide	

(Note: T=Top, B=Bottom, BT=Both)

3.5 CAD simulation

The CAD solver used to simulate and analyze the virtue prototype is SamCef Field_Oofelie. Samcef Field is the CAD used to import the iges. file and preparing the

model for simulation at Oofelie later. The imported model must undergo three pre-processes before simulating at the solver. First, the model is converted from shells to solids at modeler. For this case, there are twelve solids detected excluding the substrate and the isolation oxide. Since this CAD software is not ready to perform electromagnet signal test for RF application, so the signal path is ignored which is hidden during simulation. In other word, there is only simulation done for the mechanical path where consisting of nine solids object. The nine solids must not be combined into a big solid object although each of them are joint together in reality due to analysis data assignment later for every single part of its. Then, every solid will be assigned with all the necessary analysis data at the following stage, such as its behavior, constraint, material properties and others related data. In this stage, all of the parts will be assigned with the assembly mode which is to define they are joint with each other as multilayer supports in reality. After that, the model must be fully meshed before proceeding to the simulations stage.

Since the solver using at the laboratory is only capable in performing mechanical analysis with finite elements methods. So, there are only four types of analysis available under piezoelectric domain which is suit to be performed for this piezoelectric actuation microrelay mechanical path. Unfortunately, the CAD analyses are currently only available for some simple design, which is not involving complex geometry and multilayer structural for various types of materials. Meaning that, there is only single layer of the multilayer materials beam was simulated due to its limitation feature, and caused to have inaccuracy results. Anywhere, the results are used to compare with others in following chapter. Then further discussion on the CAD limitations in this MEMS simulation are presented in sub-section 4.5.

- **Linear Static analysis**, where it computes the static response of piezoelectric structure where an elastic field is strongly coupled with an electrical field through the material laws.

- **Modal analysis**, use to compute the eigen vibration modes of a piezoelectric structure where an elastic field is strongly coupled with an electrical field through material laws.

- **Harmonic analysis** is to computes in the frequency domain the forced response modes of a piezoelectric structure where an elastic field is strongly coupled with an electrical field through material laws.

- **Transient analysis** computes in the time domain the forced response modes of a piezoelectric structure where an elastic field is strongly coupled with an electrical field through material laws.

The potential of the electric field as well as the corresponding displacements of the mechanical field are computed for everyone of four type of analysis listed above. For other details or further information of software operating procedures and executions setting can be found at the user manual attached to it.

3.6 Additional experiment

A simple additional experiment was done in order to test the behavior of various configurations for piezo-actuator beam. Beside that, it is also used as alternative method for additional analysis due to the limitation in CAD supports at the laboratory. The main purpose of doing this test is to determine the relationship between force and displacement of the beams which is embodied in Hooke's Law which is given in equation (3.7). Beside that, it is used to estimate the force constant of various beam connections in order to verify the assumption made, such as the bridge structural driving voltage stated in sub-section 3.2.3.2.

The 30cm long plastic rulers were cut into the lengths as given in table 3.1 base on the schematic shown in figure 3.5 for the single cantilever setup and bridge structural in figure 3.6. It's representing the contact bar layer and its oxide layer, polybeam, electrodes and the piezo material. Then, they were joined by gluing each other with glue and one end clamped to fix its position. The piezoelectric force was represented by weights (F=ma) of twenty cents coins. The force was applied at middle of the beam where is stated as l_a because the curvature only occurs at l_a and l_b remaining straight

as stated in sub-section 3.2.1 by equation (3.3) previously. Firstly, single ruler without any additional layer attached to it was tested form one coin increase to five numbers of same coins. Then, it repeated for the structural as shown in figure 3.5. The measurement of the displacements was taken with the scale of a graph paper behind it, and then the readings were recorded as in table 3.2.

Table 3.1: Cantilever length ratio

	1/2 Contact	Cantilever Length		
		a	b	Total
Actual, μm	45	250	100	350
Ratio	9	20	50	79
Ruler, mm	15	33	82	130

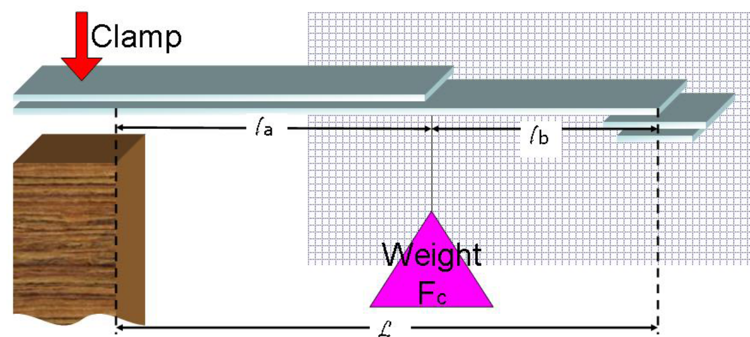

Figure 3.5: Experiment setup for cantilever beam

After that, the experiment was repeated again for bridge structural as shown in figure 3.6 and then the measurements were recorded in the same table. A graph was plotted for further analysis which is shown in following chapter section 4.2.

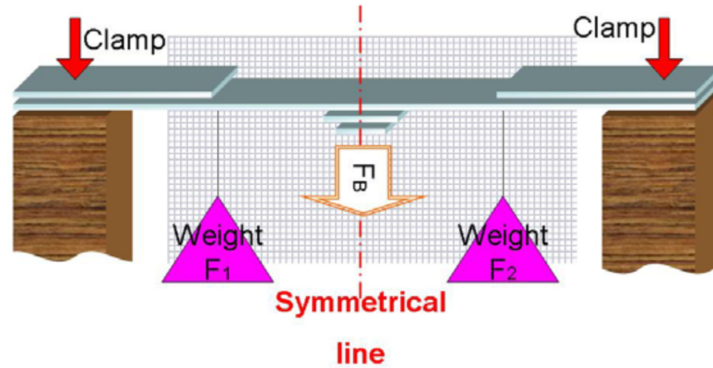

Figure 3.6: Experiment setup for bridge structural

The experiment setups involved multilayer structural for both configurations to represent the actual geometry in different scale. In this case, the piezo actuator force was represented by weight (F=ma) and the displacements were measured in block units. Based on figure 3.6, the displacements given by F_B are same as given by F_1 and F_2 ($F_B=F_1+F_2$).

Table 3.2: Experiment result

Weight F_1, F_2	F_B	Displacement	
		Cantilever	Bridge
0	0	0	0
1	2	0.5	0.1
2	4	0.9	0.3
3	6	1.3	0.5
4	8	1.5	0.7
5	10	1.9	0.8

Although, the displacement measurements for single ruler were not presented in the table, but its measurements are the greatest among them. Then, its further discussion is presented in following chapter.